Published in final edited form as:
J Mol Biol. 2012 January 27; 415(4): 759–767. doi:10.1016/j.jmb.2011.11.043.

The Receptor-CheW Binding Interface in Bacterial Chemotaxis

Anh Vu, **Xiqing Wang**, **Hongjun Zhou**, and **Frederick W. Dahlquist***
Department of Chemistry and Biochemistry, University of California Santa Barbara, Santa Barbara, CA, 93106-9510

Abstract

The basic structural unit of the signaling complex in bacterial chemotaxis consists of the chemotaxis kinase, CheA, a coupling protein, CheW, and chemoreceptors. These complexes play an important role in regulating the kinase activity of CheA and in turn controlling the rotational bias of the flagellar motor. Although individual 3D structures of CheA, CheW and chemoreceptors have been determined, yet the interaction between chemoreceptor and CheW is still unclear. We used Nuclear Magnetic Resonance (NMR) to characterize the interaction modes of chemoreceptor and CheW from *Thermotoga maritima*. We find that chemoreceptor binding surface is located near the highly conserved tip region of the N-terminal helix of the receptor, whereas the binding interface of CheW is placed between the beta-strand 8 of domain 1 and the beta-strands 1 and 3 of domain 2. The receptor-CheW complex shares a similar binding interface to that found in the "trimer of dimers" oligomer interface seen in the crystal structure of cytoplasmic domains of chemoreceptors from *Escherichia coli*. Based on the association constants inferred from fast exchange chemical shifts associated with receptor-CheW titrations, we estimate that CheW binds about 4 times tighter to its first binding site of the receptor dimer than to its second binding site. This apparent anticooperativity in binding may reflect the close proximity of the two CheW binding surfaces near the receptor tip or the further complicating the events at this highly conserved region of the receptor. This work describes the first direct observation of the interaction between chemoreceptor and CheW.

Keywords

chemotaxis; CheW; receptor; MCP; negative cooperativity

Introduction

The bacterial chemotaxis signaling system is one of the most well understood in biology. During chemotaxis, motile bacteria modulate their swimming behavior to direct their movement toward optimal environments by tracking temporal changes in chemical concentrations with high sensitivity and over a wide range of concentrations. The basic structural unit of the signaling complex in chemotaxis consists of chemotaxis kinase, CheA, coupling protein, CheW, and transmembrane receptors called methyl-accepting proteins, or MCPs. In the most completely understood receptor systems, reversible methylation and attractant ligand binding are opposing events that the signaling complexes use to regulate the

*corresponding author: dahlquist@chem.ucsb.edu, Phone: 805-893-5326, Fax: 805-893-4120.

autophosphorylation activity of CheA. This opposed modulation of kinase activity enables the cell to make comparison of the past and current environments and to control the activity of CheA in response to this comparison [1]. Once autophosphorylated, CheA transfers its phosphoryl group to the small soluble protein CheY; then CheY~P diffuses to the flagellar motor, where it binds, and enhances the switching of the flagellar motor from the counter-clockwise to clockwise rotational state.

The best understood chemotaxis receptors consist of a periplasmic domain that interacts with the appropriate target ligand, a transmembrane region followed by a HAMP domain [1] that acts as a signal conversion module, and then by a large cytoplasmic domain. The cytoplasmic portion of the receptor interacts with CheA and CheW. The cytoplasmic region of the receptor consists of a long helical region that folds back on itself to form a long two-stranded anti-parallel coiled coil. Each monomer of the receptor is assembled into dimers to form a four stranded coiled coil that seems to be the basic structural unit of the cytoplasmic region of all chemotaxis receptors [2]. To date, crystal structures of the receptor cytoplasmic domains from *E. coli* and *T. maritima* have been published. The cytoplasmic domains of all these receptors share the four stranded coiled coil structure and have a region of remarkable sequence similarity at the tip region where the individual chains fold back on themselves [2]. In Figure 1, the crystal structure of a portion of the soluble receptor TM0014 is shown in a cartoon representation of the backbone (left) where the individual polypeptide chains can be seen. Residues 90 to 206 ($TM0014_{90–206}$) are shown in a space filling representation (right) and include the conserved tip region. This receptor region has been implicated by genetic and biochemical means as the site of interaction with CheA and CheW.

CheW is a coupling protein that plays an important role in the formation of the receptor – signaling complex. It contains two β sheet domains. Each domain consists of a five-stranded β –barrel that forms an internal hydrophobic core for protein – protein interaction. Its structure is quite similar to that of CheA P5 domain and it is known that they interact with each other.

There have been several studies on the interaction of the chemoreceptor complexes with other chemotactic proteins; [9]. Although the crystal structure of CheA containing the CheW and receptor coupling domains (P4P5) in *T. maritima* has been solved [4], the interaction between the chemoreceptors and CheW is still unclear. The 3D structures of CheW and TM0014 have been solved by NMR and X-ray crystallography respectively. The chemotaxis proteins from *T. maritima* are well-behaved at millimolar concentration and are stable at up to 90°C. This makes them well suited for structural analysis by solution nuclear magnetic resonance (NMR) methods. Here, we report the identification of a binding interface between chemoreceptor TM0014 and CheW from *T. maritima* using NMR methods.

Results

TM0014 is a soluble receptor without the transmembrane regions [10]. Each monomer in the four-helix bundle dimer has 213 residues. The extended shape of this protein makes its effective size significantly larger than a globular protein of comparable molecular weight. Its rotational diffusion properties are unfavorable for detailed NMR studies of the backbone of the dimer. To facilitate high-resolution NMR study of the receptor backbone, we constructed a shorter fragment of the receptor, $TM0014_{90–206}$, that contains the helix bundle tip region of the full-length receptor, and a 5 His tag, and an additional tyrosine residue (used to determine protein concentration) at its N-terminus. As expected, the tyrosine mutant and $TM0014_{90–206}$ both showed the same chemical shift perturbation in the ^{1}H-^{15}N TROSY-HSQC spectra upon addition of CheW, confirming that the tyrosine mutant does not perturb the CheW-receptor interaction.

Sequential assignment of the receptor fragment

The backbone amide assignments of the receptor fragment $TM0014_{90–206}$ were completed using TROSY-based HNCACB, HNCA, HNCOCA, and HNCOCACB experiments (see Experimental Procedures). We used U-[^{2}H,^{15}N,^{13}C]-labeled $TM0014_{90–206}$ for the backbone assignment. Figure 2a showed the assigned ^{1}H-^{15}N TROSY-HSQC spectrum of $TM0014_{90–206}$. The backbone amide resonances of $TM0014_{90–206}$ were well dispersed with mostly sharp resonances at 40°C. A total of 6 residues were unassigned because we were not able to detect their backbone amide resonances in the 3D spectra. These residues were Lys90, Ser91, Gly92, Thr93, and Asn 94 at the N-terminus, and Glu149 located right at the center of the tip region. The missing resonances of Lys90, Ser91, Gly92, Thr93, Asn 94, and Glu149 could be due to dynamic effects of conformational heterogeneity and/or solvent-exchange effects. Figure 2b shows a plot of chemical shift index[10] as a function of residue number. As can be seen in the figure, the secondary structure of the fragment is largely helical with a distinct break at residues 146–151 corresponding to the position where the polypeptide chain folds back on itself to form the tip of the receptor.

The receptor binding interface of CheW

We performed chemical-shift-perturbation mapping with {[U-^{2}H,^{12}C], $Ile_{\gamma1}$-[$^{13}CH_3$], Leu,Val-[$^{13}CH_3$]}-labeled[12] but otherwise deuterated CheW by titrating it with protonated and deuterated $TM0014_{90–206}$ and TM0014. The CheW interface residues are identified by comparing the spectra collected with a protonated partner and a deuterated partner[13]. Figure 3a shows the Ile, Leu and Val methyl side chain spectrum of {[U-^{2}H,^{12}C], $Ile_{\gamma1}$-[13CH_3], Leu,Val-[13CH_3]}-labeled CheW in the presence of an excess of deuterated $TM0014_{90–206}$. Comparing the isoleucine, valine, and leucine methyl group spectra of CheW alone (black) and CheW in the presence of $TM0014_{90–206}$ (red), respectively, we observed residue specific chemical shift changes in CheW upon binding $TM0014_{90–206}$. Essentially identical chemical shift changes were observed when we added an excess of intact TM0014 to the methyl labeled CheW (Supplement data S1), showing that the shorter receptor construct contains the same binding site for CheW as the intact receptor. The methyl resonances of CheW residues Val27 and Val98 broadened greatly when bound to protonated $TM0014_{90–206}$ but were sharper and could be observed at higher saturation with deuterated receptor. This difference in broadening between using the protonated and deuterated versions of $TM0014_{90–206}$, most likely reflects the proximity of the valine methyl groups of CheW to protons on the receptor[13]. The strongly distance dependent dipolar broadening is reduced when the protons of the receptor are replaced by deuterons.

Resonances from other neighboring residues, including Leu14, Ile30 and Leu99, also shifted moderately in the presence of $TM0014_{90–206}$. The largest chemical shift changes were localized in one hydrophobic patch on CheW, as illustrated in the surface representation of CheW shown in Figure 3d. The residues of CheW with the largest shifts, and the residues with more moderate shifts, were colored red and yellow, respectively. As can be seen, significant changes in chemical shift were observed in residues located in β-strands 1–3 and 8 of CheW. We assayed the binding affinity of CheW in the presence of $TM0014_{90–206}$ by plotting the chemical shift perturbation of a given resonance from its free position by different concentrations of $TM0014_{90–206}$. Several peaks shifted progressively as the receptor fragment was added, showing that the binding was in the fast exchange regime. The titration curve for Val98 was shown in Figure 3c as a plot of the observed chemical shift of the methyl resonance of Val98 as a function of $TM0014_{90–206}$ concentration. These data were fitted to a hyperbolic binding isotherm, and the dissociation constant was determined to be ~ 300 uM.

The CheW binding interface ot TM0014$_{90–206}$

The binding surface of TM0014$_{90–206}$ in contact with CheW was observed, using a series of ^{1}H-^{15}N TROSY-HSQC spectra of TM0014$_{90–206}$ taken over the course of a titration with CheW. Figure 4a showed the superimposition of two ^{1}H-^{15}N HSQC spectra of TM0014$_{90–206}$ (black) and TM0014$_{90–206}$-CheW complex (red). Significant chemical shift changes were observed in TM0014$_{90–206}$ due to the binding of CheW. The backbone amide resonances of residues 132, 137, 139, 140, 141, 142, 143, 145, 146 and 156 of TM0014$_{90–206}$ shifted significantly when associated with CheW. It should be noted that the backbone amide of residue 135 did not shift significantly but its methyl resonance did shift (not shown). Figure 4b showed the observed chemical shift perturbation for each assigned residue of TM0014$_{90–206}$ as a plot of the observed chemical shift change as a function of residue number. Significant chemical shift changes were localized in one area of TM0014$_{90–206}$. Figure 4d showed the residues, with observed combined chemical shift changes above 30 Hz, colored red on the crystal structure of TM0014. These residues formed a well-defined hydrophobic patch at the tip region of TM0014 and were exposed to the solvent where CheW can interact. We estimated the strength of the CheW-receptor interaction by plotting the observed chemical shift of the methyl resonance peak of Ile135 as a function of CheW concentration in Figure 4c. The curve suggested a dissociation constant of ~1.2 mM.

As shown from the data presented in Figure 3, the NMR based titration of labeled CheW by unlabeled receptor fragment suggests an affinity about four fold stronger than is observed when labeled receptor is titrated with unlabeled CheW. This discrepancy is well outside of experimental error and reflects the stoichiometry and nature CheW-receptor interaction. When CheW is titrated by excess receptor fragment, the binding is predominated by one CheW bound per receptor dimer. However, when receptor fragment is titrated by excess CheW, the binding now reflects a combination of both one and two CheW molecules bound per receptor dimer. If each monomer of the receptor dimer bound CheW identically and independently of whether a CheW was bound at the other monomer, both titrations should show the same apparent affinity. However, if the binding of the first CheW results in a lower affinity for the binding of the second, it would require a higher CheW concentration to fully saturate the receptor dimer than the concentration of receptor needed to saturate CheW. This is exactly what is observed.

Discussion

Our results suggest that TM0014$_{90–206}$ retains the native structure of intact TM0014. Static light scattering data (not shown) confirm the dimer nature of the shortened version of TM0014 as expected. The chemical shift index results demonstrate that the secondary structure of TM0014$_{90–206}$ consists of two helices with a distinct break at residues 146–151, in agreement with the crystal structure of TM0014. When we superimpose the isoleucine methyl side chain spectrum of TM0014 with TM0014$_{90–206}$ (Supplement data S2), TM0014$_{90–206}$ shows a subset of the resonances observed for TM0014. This suggests that TM0014 and TM0014$_{90–206}$ share a common structure. The TM0014 construct was shortened further to form TM0014$_{107–191}$. TM0014$_{107–191}$ has a very different isoleucine methyl chemical shift spectrum when compared to the other two fragments (Supplement data S2). In addition, TM0014$_{107–191}$ is not as stable as TM0014$_{90–206}$ and TM0014 and TM0014$_{107–191}$ tends to precipitate at high concentration. This suggests that the length of the receptor plays an important role in maintaining the conformation of the tip region as well as providing structural stability.

In this study, we have identified the interaction interfaces of TM0014$_{90–206}$ and CheW complex in solution by chemical shift perturbation techniques. The receptor interaction

surface of CheW consists of residues located in the solvent-exposed patches of β strands 1, 3, and 8 as summarized in Figure 3d. The presence of TM0014 or $TM0014_{90–206}$ cause similar methyl chemical shift changes in the HMQC spectra of CheW (see supplemental data). This confirms that the binding of $TM0014_{90–206}$, and CheW has not been affected by shortening the TM0014 fragment. Previous studies from genetic suppressor screens and biochemical assays suggested residues of *E. coli* CheW to be important for interaction with the receptors. These homologous residues are also involved in the interaction between CheW and receptor in *T. maritima*, consistent with the high degree of structural similarity, although their amino acid sequences were not very similar [3,14].

The CheW interaction surface of $TM0014_{90–206}$ has been identified and consists mainly of residues near or at the tip region, on the N-terminal side of the tip of the receptor (N-terminal helix). A few residues near the hairpin loop on the C-terminal side (C-terminal helix) of the receptor showed small chemical shift changes when CheW was added. This suggests that the residues on the N-terminal side play major role whereas the residues on the C-terminal side play a more minor role in the receptor and CheW interaction. Lui and Parkinson [7] determined a few suppressor mutation sites on the receptors, including two residues located near our proposed binding sites. Mehan et al. [9] used chemical modifications to map regions of the *E. coli* receptor Tar that interfered with normal regulation of CheA and found a sub-population of sites near the receptor tip that inhibited activation of CheA in the presence of CheW. These are in similar locations to those we have identified in $TM0014_{90–206}$ A recent study by Mowery et al.[15] showed that all R366 mutants of Tsr, which are equivalent to R146 of $TM0014_{90–206}$, either impaired or destroyed Tsr function, possibly by disrupting the interaction of the receptor and CheW and in turn prevented the formation of the signaling complexes. This evidence seems to agree well with the chemical shift perturbation studies.

Currently there are two predominant structural models for receptor-receptor interaction in an extended signaling network; the trimer of dimers model, based on crystal packing of the *E. coli* serine receptor cytoplasmic domain [16], and the hedge row of dimers model based on the crystal packing of a *T. maritima* receptor cytoplasmic domain [4]. The trimer of dimers model has been generally supported by electron tomography [17,18], genetic studies [19], and biochemical analysis [20,21,22]. Recently, there has been a report about the universal architecture of chemoreceptor array among many bacteria, including *T. maritima* [18], that favors the hexagonal symmetry, the trimers of dimers model. In addition, a series of recent studies from the Hazelbauer laboratory suggests that trimers of receptor dimers are critical for receptor function [23,24,25] in the *E. coli* system. The preponderance of current evidence supports the trimer of dimers view of receptor organization.

Analysis from the Parkinson laboratory [19] suggests that there are 11 principal trimer contact residues that are highly conserved among chemotactic bacteria. Somewhat surprisingly, 6 of those 11 trimer contact residues are also involved in the receptor and CheW interaction based on our NMR results. These residues were mapped onto the 3D structure of the cytoplasmic domain of Tsr in the trimer of dimer arrangement. In Figure 5, one can see that these residues are also involved in the receptor interaction. This implies that the trimer interface shares similar contact regions with the receptor and CheW. Earlier evidence by Studdert and Parkinson supported this idea. They demonstrated that the presence of CheW and CheA prevented the exchange between members with recently made receptor molecules and stabilized the trimer formation [21]. One explanation could be that the principal trimer contact is blocked by CheW binding to receptors and the formation of trimers of dimers as well as the interaction between the receptor and CheW are a competitive process. Recently, Cardozo et al. showed that over-expression of CheW in *E. coli* cells, resulted in disruption

of receptor arrays [26], supporting the notion that CheW binding and trimer formation are competitive processes.

The remarkable sequence conservation observed at the tip of chemotaxis receptors in virtually all motile bacteria is not seen in CheW. CheW homologs show multiple substitutions throughout the sequence, although these changes are generally conservative. This suggests that the receptor tips have a more complex biochemical role, involving receptor array assembly as well as simple binding interactions with CheW and CheA. Previous studies have revealed that most mutants at the tip of the *E. coli* serine receptor are defective in their ability to mediate chemotactic responses, but it has not been easy to assign one simple biochemical defect to these mutations [19].

The apparent negative cooperativity we observe in CheW binding suggests that there might be steric hindrance caused by CheW binding to the first binding site of the receptor, which makes it difficult to fit another CheW on the second binding site of the receptor at the relatively small receptor tip. It is also possible that when the first CheW binds, it might produce structural changes to the second binding site that result in lowered affinity. Alternatively, since the P5 domain of CheA is structurally homologous to CheW [2,5], one of the CheW binding sites on the receptor might be the true binding surface for CheW, while the weaker binding we see could represent the binding surface for the CheA P5 domain on the receptor. The relatively low affinity of the first binding is in contrast to that seen in the *E. coli* system, where CheW appears to bind much more strongly to the chemotaxis receptors [27]. This affinity difference is reversed when considering the CheW – CheA interaction. *Thermotoga* CheW binds much more strongly to its CheA than does the *E. coli* CheW to its CheA. It remains unclear what the physiological consequences might be of these differences in affinity and what role the apparent negative cooperativity we observe may have on the signaling properties of the receptor-CheA-CheW complex.

Experimental Procedures

Protein expression and purification

Sample Preparation—The TM0014 construct was received from Brian Crane's laboratory. PCR methods were used to generate a DNA fragment encoding TM0014 from Lys90 to Thr206 to create a $TM0014_{90–206}$ construct. The DNA encoding $TM0014_{90–206}$ was subcloned into the vector pET28a (Novagen), and the N-terminal histidine of the his tag was mutated to tyrosine using QuickChange mutagenesis (Stratagene). $TM0014_{90–206}$ proteins with an N-terminal His_5 tags were transformed and over expressed in *E. coli* strain BL21(RIL DE3) (Novagen). During the log phase of bacterial growth, isopropyl β-D-thiogalactopyranoside (IPTG) was added at 1mM concentration. U-[^{15}N,^{13}C,^{2}H] - labeled $TM0014_{90–206}$ were grown in minimal media which consisted of 1 mM magnesium sulfate, 0.1 mM calcium chloride, 0.5 μg/ml of thiamine, and 100 μg/ml of ampicillin, with the addition of 1g/L of $^{15}NH_4Cl$ as the main nitrogen source, and 2g/L U[^{13}C,^{2}H]-glucose or 2g/L of U-[^{12}C,^{2}H]-glucose (CIL, Andover, MA) as the main carbon source. {[U-^{2}H,^{12}C], $Ile_{\gamma}1$-[13CH3]}-labeled TM001490-206 and TM0014 and {[U-^{2}H,^{12}C], $Ile_{\gamma}1$-[13CH3], Leu,Val_{δ}-[13CH3]}-labeled CheW were prepared using the method previously described by Kay laboratory [12]. His_5-tagged $TM0014_{90–206}$ was purified using nickel affinity column (Ni-NTA Agarose, QIAGEN) and size exclusion chromatography. CheW was over expressed and purified as previously described [3]. Purified proteins were dialyzed in 50mM Na_2HPO_4 and 1mM EDTA at pH 7.4. All NMR samples contained 0.02% sodium azide and 10% D_2O.

NMR data collection and processing—NMR data were collected at 40°C on a Varian 600Mhz or a Bruker 800Mhz spectrometer, each using a ^{1}H/^{13}C/^{15}N/^{2}H cryogenically

cooled probe equipped with a Z pulsed-field gradient. Sequential assignments of $TM0014_{90–206}$ were accomplished with a U-[^{15}N,^{13}C,^{2}H] sample of $TM0014_{90–206}$, using TROSY b ased 2D Heteronuclear Single Quantum Coherence (HSQC) and TROSY based 3D triple resonance HNCACB [28,29,30], HN(CO)CACB, HNCA [28,29,31,32,33] and HN(CO)CA experiments [34]. All titration experiments were performed. In the first titration, 300 μM {[U-^{2}H,^{12}C], $Ile_{\gamma1}$-[$^{13}CH_3$]}-labeled $TM0014_{90–206}$ was titrated with ^{2}H-labeled CheW to a concentration between 0 and 1500 μM. At each titration point a Heteronuclear Multiple Quantum Coherence (HMQC) spectrum was collected at 40C. The same titration was repeated with 300 μM {[U-^{2}H,^{12}C], $Ile_{\gamma1}$-[$^{13}CH_3$], Leu,Val_{δ}-[$^{13}CH_3$]}-labeled CheW mixed with varying concentrations of [U-^{2}H]-labeled $TM0014_{107–191}$ between 0 and 1500 μM. The titration analysis was done assuming fast exchange using one to one binding of CheW to $TM0014_{90–206}$ monomer units to form the CheW - $TM0014_{90–206}$ complex. ^{1}H-^{13}C HMQC spectra were collected at CheW: $TM0014_{90–206}$ molar ratios of 0, 0.50, 0.75, 1.0, 2.0, 3.0, 4.0, and 5.0 when methyl $TM0014_{90–206}$ spectra were observed. A similar titration was performed to obtain methyl CheW spectra with $TM0014_{90–206}$:CheW molar ratios of 0, 0.50, 0.75, 1.0, 2.0, 3.0, and 4.0. Binding constants were estimated by fitting the observed population-weighted displacement of the resonance peaks from free to bound states during the titration.

Supplementary Material

Refer to Web version on PubMed Central for supplementary material.

Acknowledgments

We thank Brian Crane and Abiola Pollard (Cornell University) for the TM0014 construct. Robert Levenson provided discussion and technical advice. This work was support by NIH grant GM59544 to FWD.

References

1. Hazelbauer GL, Falke JJ, Parkinson JS. Bacterial chemoreceptors: high-performance signaling in networked arrays. Trends Biochem Sci. 2008; 33:9–19. [PubMed: 18165013]
2. Alexander RP, Zhulin IB. Evolutionary genomics reveals conserved structural determinants of signaling and adaptation in microbial chemoreceptors. Proc Natl Acad Sci U S A. 2007; 104:2885–90. [PubMed: 17299051]
3. Griswold IJ, Zhou H, Matison M, Swanson RV, McIntosh LP, Simon MI, Dahlquist FW. The solution structure and interactions of CheW from Thermotoga maritima. Nat Struct Biol. 2002; 9:121–5. [PubMed: 11799399]
4. Park SY, Borbat PP, Gonzalez-Bonet G, Bhatnagar J, Pollard AM, Freed JH, Bilwes AM, Crane BR. Reconstruction of the chemotaxis receptor-kinase assembly. Nat Struct Mol Biol. 2006; 13:400–7. [PubMed: 16622408]
5. Boukhvalova MS, Dahlquist FW, Stewart RC. CheW binding interactions with CheA and Tar. Importance for chemotaxis signaling in Escherichia coli. J Biol Chem. 2002; 277:22251–9. [PubMed: 11923283]
6. Boukhvalova M, VanBruggen R, Stewart RC. CheA kinase and chemoreceptor interaction surfaces on CheW. J Biol Chem. 2002; 277:23596–603. [PubMed: 11964403]
7. Liu JD, Parkinson JS. Genetic evidence for interaction between the CheW and Tsr proteins during chemoreceptor signaling by Escherichia coli. J Bacteriol. 1991; 173:4941–51. [PubMed: 1860813]
8. Liu JD, Parkinson JS. Role of CheW protein in coupling membrane receptors to the intracellular signaling system of bacterial chemotaxis. Proc Natl Acad Sci U S A. 1989; 86:8703–7. [PubMed: 2682657]
9. Mehan RS, White NC, Falke JJ. Mapping out regions on the surface of the aspartate receptor that are essential for kinase activation. Biochemistry. 2003; 42:2952–9. [PubMed: 12627961]

10. Pollard AM, Bilwes AM, Crane BR. The structure of a soluble chemoreceptor suggests a mechanism for propagating conformational signals. Biochemistry. 2009; 48:1936–44. [PubMed: 19149470]
11. Wishart DS, Sykes BD, Richards FM. The chemical shift index: a fast and simple method for the assignment of protein secondary structure through NMR spectroscopy. Biochemistry. 1992; 31:1647–51. [PubMed: 1737021]
12. Tugarinov V, Kay LE. An isotope labeling strategy for methyl TROSY spectroscopy. J Biomol NMR. 2004; 28:165–72. [PubMed: 14755160]
13. Hamel DJ, Dahlquist FW. The contact interface of a 120 kD CheA-CheW complex by methyl TROSY interaction spectroscopy. J Am Chem Soc. 2005; 127:9676–7. [PubMed: 15998058]
14. Li Y, Hu Y, Fu W, Xia B, Jin C. Solution structure of the bacterial chemotaxis adaptor protein CheW from Escherichia coli. Biochem Biophys Res Commun. 2007; 360:863–7. [PubMed: 17631272]
15. Mowery P, Ostler JB, Parkinson JS. Different signaling roles of two conserved residues in the cytoplasmic hairpin tip of Tsr, the Escherichia coli serine chemoreceptor. J Bacteriol. 2008; 190:8065–74. [PubMed: 18931127]
16. Kim KK, Yokota H, Kim SH. Four-helical-bundle structure of the cytoplasmic domain of a serine chemotaxis receptor. Nature. 1999; 400:787–92. [PubMed: 10466731]
17. Zhang P, Khursigara CM, Hartnell LM, Subramaniam S. Direct visualization of Escherichia coli chemotaxis receptor arrays using cryo-electron microscopy. Proc Natl Acad Sci U S A. 2007; 104:3777–81. [PubMed: 17360429]
18. Briegel A, Ortega DR, Tocheva EI, Wuichet K, Li Z, Chen S, Muller A, Iancu CV, Murphy GE, Dobro MJ, Zhulin IB, Jensen GJ. Universal architecture of bacterial chemoreceptor arrays. Proc Natl Acad Sci U S A. 2009; 106:17181–6. [PubMed: 19805102]
19. Ames P, Studdert CA, Reiser RH, Parkinson JS. Collaborative signaling by mixed chemoreceptor teams in Escherichia coli. Proc Natl Acad Sci U S A. 2002; 99:7060–5. [PubMed: 11983857]
20. Studdert CA, Parkinson JS. Insights into the organization and dynamics of bacterial chemoreceptor clusters through in vivo crosslinking studies. Proc Natl Acad Sci U S A. 2005; 102:15623–8. [PubMed: 16230637]
21. Studdert CA, Parkinson JS. Crosslinking snapshots of bacterial chemoreceptor squads. Proc Natl Acad Sci U S A. 2004; 101:2117–22. [PubMed: 14769919]
22. Parkinson JS, Ames P, Studdert CA. Collaborative signaling by bacterial chemoreceptors. Curr Opin Microbiol. 2005; 8:116–21. [PubMed: 15802240]
23. Li M, Hazelbauer GL. Core unit of chemotaxis signaling complexes. Proc Natl Acad Sci U S A. 2011; 108:9390–5. [PubMed: 21606342]
24. Li M, Khursigara CM, Subramaniam S, Hazelbauer GL. Chemotaxis kinase CheA is activated by three neighbouring chemoreceptor dimers as effectively as by receptor clusters. Mol Microbiol. 2011; 79:677–85. [PubMed: 21255111]
25. Boldog T, Li M, Hazelbauer GL. Using Nanodiscs to create water-soluble transmembrane chemoreceptors inserted in lipid bilayers. Method Enzymol. 2007; 423:317–35.
26. Cardozo MJ, Massazza DA, Parkinson JS, Studdert CA. Disruption of chemoreceptor signalling arrays by high levels of CheW, the receptor-kinase coupling protein. Mol Microbiol. 2010; 75:1171–81. [PubMed: 20487303]
27. Gegner JA, Graham DR, Roth AF, Dahlquist FW. Assembly of an MCP receptor, CheW, and kinase CheA complex in the bacterial chemotaxis signal transduction pathway. Cell. 1992; 70:975–82. [PubMed: 1326408]
28. Salzmann M, Pervushin K, Wider G, Senn H, Wuthrich K. [13C]-constant-time [15N,1H]-TROSY-HNCA for sequential assignments of large proteins. J Biolmol NMR. 1999; 14:85–8.
29. Loria JP, Rance M, Palmer AG 3rd. Transverse-relaxation-optimized (TROSY) gradient-enhanced triple-resonance NMR spectroscopy. J Magn Reson. 1999; 141:180–4. [PubMed: 10527755]
30. Meissner A, Sorensen OW. Sequential HNCACB and CBCANH protein NMR pulse sequences. J Magn Reson. 2001; 151:328–31. [PubMed: 11531355]

31. Salzmann M, Pervushin K, Wider G, Senn H, Wuthrich K. TROSY in triple-resonance experiments: new perspectives for sequential NMR assignment of large proteins. Proc Natl Acad Sci U S A. 1998; 95:13585–90. [PubMed: 9811843]

32. Pervushin K, Gallius V, Ritter C. Improved TROSY-HNCA experiment with suppression of conformational exchange induced relaxation. J Biomol NMR. 2001; 21:161–6. [PubMed: 11727979]

33. Salzmann M, Wider G, Pervushin K, Wuthrich K. Improved sensitivity and coherence selection for [15N,1H]-TROSY elements in triple resonance experiments. Journal of Biomolecular NMR. 1999; 15:181–4. [PubMed: 10605091]

34. Yang D, Kay LE. Improved lineshape and sensitivity in the HNCO-family of triple resonance experiments. J Biomol NMR. 1999; 14:273–276.

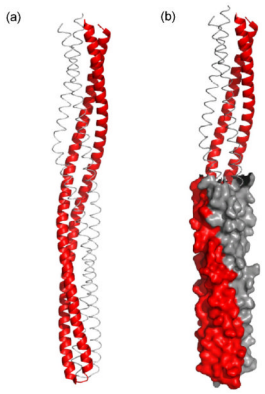

Figure 1.
Ribbon and worm diagrams of the structure of TM0014 (a) showing the two monomer chains (red and gray). (b) A representation of the short construct $TM0014_{90–206}$ in a space-filling view (red and gray) using the coordinates of TM0014. The ribbon and worm representations show those residues deleted in the shortened construct.

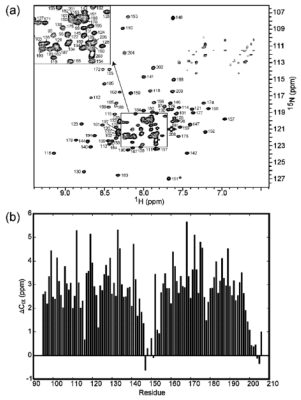

Figure 2.

The assigned ^{1}H-^{15}N TROSY HSQC spectrum and the secondary structure analysis of TM0014$_{90–206}$. (a) ^{1}H-^{15}N correlation map of ^{15}N-labeled TM0014$_{90–206}$ from *T. maritima* collected at 40°C and pH 7.4. The assignment of backbone amides is indicated with sequence numbers. Asterisks indicate aliasing of the peaks from outside the spectral window along ^{15}N dimension. The central region enclosed by the square is expanded and represented as a small section in the upper left corner of the spectrum. (b) The differences between the observed Cα chemical shifts of residues 90–206 and their respective random-coil chemical shifts were plotted as a function of residue number. Continuous stretches of positive ΔC_α are indicative of helices, while the small stretches with both positive and negative ΔC_α values at residues 146–151 are suggestive of loops.

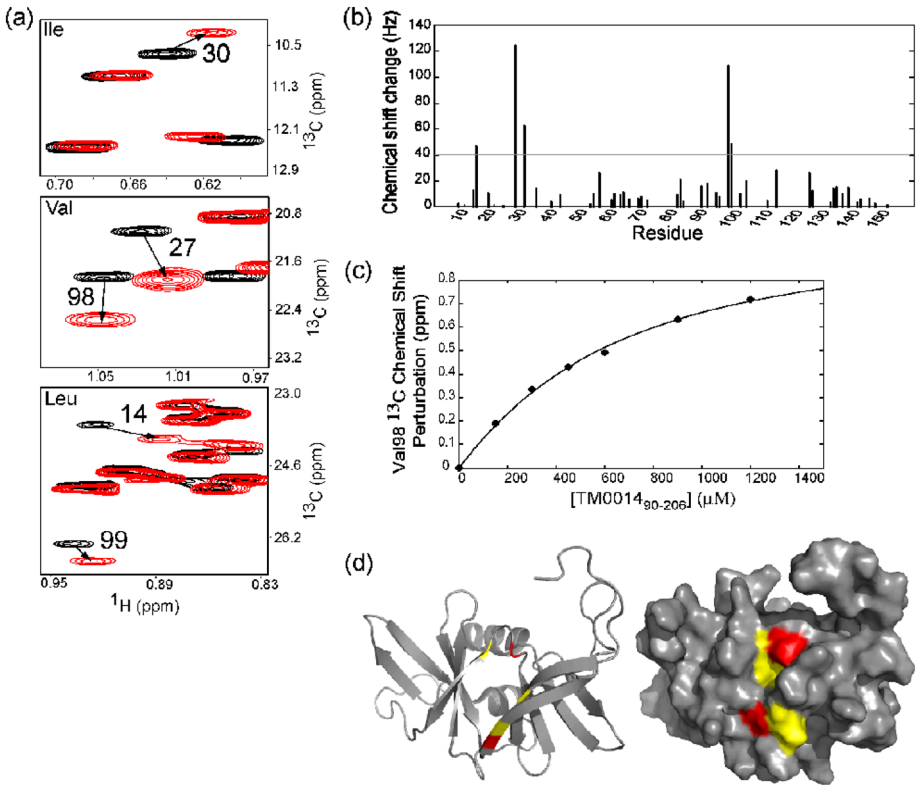

Figure 3.

The interaction between the coupling protein CheW and the soluble receptor fragment TM0014$_{90–206}$. (a) A superimposition of ^{1}H-^{13}C HMQC spectra of ILV methyl groups of CheW (black) and CheW in the presence of TM0014$_{90–206}$ (red). Residues with significant chemical shifts are numbered with the arrows indicating the direction of the shift. (b) Measured chemical shift perturbations of CheW by the presence of receptor as a function of residue number represented as combined chemical shift $(\Delta H^2+\Delta N^2)^{1/2}$ in hertz. (c) Changes in chemical shift of V98 of CheW by TM0014$_{90–206}$. The calculated binding curve is shown with a best-fit dissociation constant of 300 μM. (d) TM0014$_{90–206}$ binds to a hydrophobic surface of CheW, formed by β-strands 1, 2, 3, and 8 and the loop bridging β-strands 2 and 3. The residues the showing the largest chemical shift changes are shown in red (residues 27 and 98) and the residues with moderate shifts are shown in yellow (residues 14, 30 and 99).

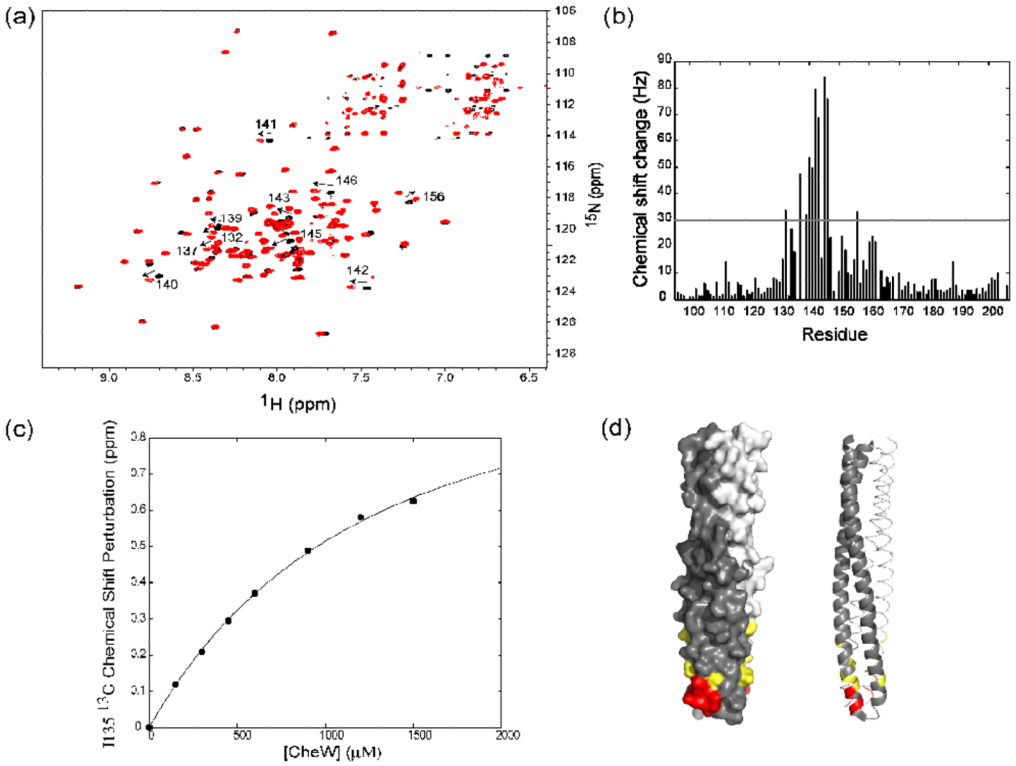

Figure 4.

The interaction of $TM0014_{90–206}$ with the coupling protein CheW. (a) A superimposition of ^{1}H-^{15}N TROSY HSQC spectra of $TM0014_{90–206}$ (black) and $TM0014_{90–206}$ in the presence of CheW (red). Large chemical-shift changes (indicated by arrows), are seen in the tip region of the receptor (residues 132, 137, 139, 140, 141, 142, 143, 145, 146, and 156). (b) Measured combined chemical shifts changes in the presence of CheW plotted as a function of residue number for $TM0014_{90–206}$. (c) Changes in chemical shift of $TM0014_{90–206}$ as a function of CheW concentration. The calculated binding curve is shown for residue 135 with best-fit dissociation constant of 1200 μM. (d) Mapping of the residues of $TM0014_{90–206}$ perturbed upon binding of CheW on the structure $TM0014_{90–206}$. Residues with chemical shifts larger than 50 Hz are shown in red; those with shifts between 30 and 50 Hz are shown in yellow.

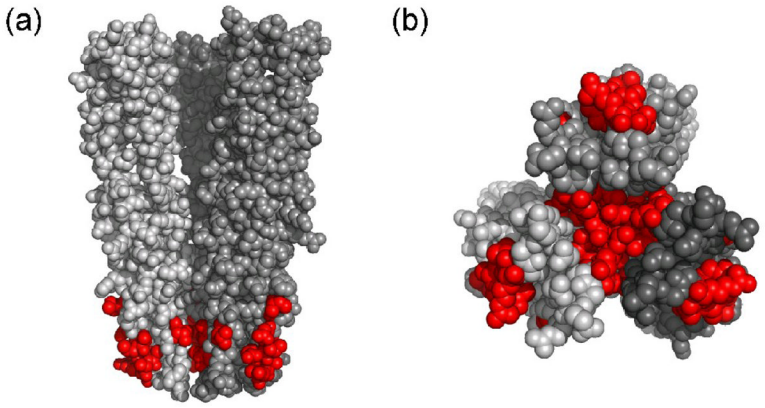

Figure 5.

Mapping of contact residues of TM0014$_{90–206}$ that are involved in the CheW interaction (red) onto the 3D crystal structure of *E. coli* trimer of dimer Tsr receptor. (a) Space-filling side view of cytoplasmic domain of Tsr residues 335–446 in the trimer of dimer arrangement. Residues 377, 381, 384, 385, 388, 398 of Tsr correspond to residues 135, 139, 142,143, 146, and 156 of TM0014. (b) A bottom view of the space-filling model of the trimer of dimers.